Live Load Radial Moment Distribution for Horizontally Curved Bridges

Woo Seok Kim[1]; Jeffrey A. Laman[2]; and Daniel G. Linzell[3]

Abstract: The present study is designed to determine the effect of major parameters on maximum total bending moments of curved girders, establish the relationship between key parameters and girder distribution factors (GDFs), and develop new approximate distribution factor equations. A level of analysis study using three numerical models was performed to establish an appropriate numerical modeling method on the basis of field test results. A total of 81 two-traffic lane curved bridges were analyzed under HL-93 loading. Two approximate GDF equations were developed based on the data obtained in this study: (1) a single GDF based on total girder normal stress; and (2) a combined GDF treating bending and warping normal stress separately. The two equations were developed based on both an averaged coefficient method and regression analysis. A goodness-of-fit test revealed that the combined GDF model developed by regression analysis best predicted GDFs. The present study demonstrated that radius, span length, cross frame spacing and girder spacing most significantly affect GDFs. The proposed GDF equations are expected to provide a more refined live load analysis for preliminary design.

DOI: 10.1061/(ASCE)1084-0702(2007)12:6(727)

CE Database subject headings: Bridges, steel; Live loads; Curvature; Load distribution; Finite element method.

Introduction

The present study was initiated to establish new, approximate girder distribution factors (GDF) equations for design of horizontally curved steel I-girder bridges. In order to design or evaluate a bridge, the maximum girder moment must be predicted. The use of approximate GDFs to distribute vehicle loading to individual girders offers a simple method to either proceed with design or complete an approximate analysis. After maximum girder moments are determined using GDFs, each girder can be designed as an isolated girder. In AASHTO LRFD (2006), the GDF for a straight girder is defined as a function of girder spacing, span length, slab thickness, and girder stiffness. However, the *AASHTO Guide* (1993) GDF equation for curved bridges includes only girder spacing, span length, and curvature. *AASHTO Guide* (2003) excludes the GDF equation because more accurate GDFs are still required.

Horizontally curved girders experience significant normal stresses due to warping torsion that are superimposed onto normal stresses induced by bending in a vertical plane. Cross frames are designed to resist significant girder torsional moments along with providing lateral support to the girder, therefore, cross frames become primary load carrying members and integral to the behavior of the structure under live and dead loads. The presence of cross frames does not eliminate the torsional moment induced in the girders, but, mitigates warping normal stresses by providing torsional restraint to the girders at regular intervals. Cross frames also influence vertical bending stress distribution by providing an additional load path between the curved girders. Hence, cross frame spacing affects both torsional moments and radial distribution of vertical bending moments. Therefore, it must be a variable considered in the development of a GDF equation to accurately predict curved girder moments and, therefore, stresses. Available approximate radial moment distribution equations from *AASHTO Guide* (1993) or previous research are not a function of cross frame spacing and, therefore, predict girder flange normal stresses with less accuracy than is possible. Therefore, the present study develops practical, approximate GDF equations for horizontally curved I-girder bridges that include key, available bridge geometric parameters. Results reported herein indicate that the proposed GDF equations result in improved accuracy over previously reported equations.

Objectives and Scope

Because testing of in-service bridges requires extensive resources and prediction models developed from field tests are limited to the particular geometry of the tested bridge, the present research employs a numerical approach verified using available field data. All numerical analyses were conducted within a geometrically linear range and excluded material nonlinearity. To reduce the number of numerical analyses that were performed, the present study involved limited independent parameters and a fixed bridge cross section. The chosen bridge cross section consisted of a simply supported, four curved girder steel superstructure supporting a concrete slab which contained two-traffic lanes. The cross section has no superelevation of the deck and no vertical curve was in-

[1]Research Assistant, Dept. of Civil and Environmental Engineering, The Pennsylvania State Univ., University Park, PA 16802. E-mail: wuk106@psu.edu

[2]Associate Professor, Dept. of Civil and Environmental Engineering, The Pennsylvania State Univ., University Park, PA 16802. E-mail: jlaman@psu.edu

[3]Associate Professor, Dept. of Civil and Environmental Engineering, The Pennsylvania State Univ., University Park, PA 16802. E-mail: dlinzell@engr.psu.edu

Note. Discussion open until April 1, 2008. Separate discussions must be submitted for individual papers. To extend the closing date by one month, a written request must be filed with the ASCE Managing Editor. The manuscript for this paper was submitted for review and possible publication on December 16, 2005; approved on September 12, 2006. This paper is part of the ***Journal of Bridge Engineering***, Vol. 12, No. 6, November 1, 2007. ©ASCE, ISSN 1084-0702/2007/6-727–736/$25.00.

Table 1. Key Parameters Ranges

Parameter	Range [m (ft)]
Radius	61, 107, 229 (200, 350, 750)
Girder spacing	3.05, 3.35, 3.66 (10, 11, 12)
Span length	22, 33, 44 (72, 108, 144)
Cross frame spacing	2.2, 3.7, 5.5 (7.2, 12, 18)

cluded along the span because it was not expected to significantly affect the GDFs. The standard HL-93 truck load model was used in conjunction with AASHTO LRFD (2006) multiple presence factors.

Preliminary Studies to Determine Scope: Design parameters expected to influence radial distribution of moment were investigated to establish key parameters. The effect of continuous concrete parapets, concrete deck thickness, girder web depth and flange width were evaluated and determined to have very small or insignificant influence on the radial distribution. These parameters were, therefore, excluded from the parametric study. The key parameters determined by the present research were bridge radius, girder spacing, bridge span length, and cross frame spacing. The range of the four selected key parameters is presented in Table 1, resulting in 81 cases for the parametric study. Concrete deck thickness was modeled consistently in each of the numerical models used in the parametric study. In addition, X-type cross frames and a constant concrete deck overhang length were modeled in each of the 81 cases.

The primary objectives of the present study are to: (1) verify the relationship of key parameters and GDFs using a parametric study and statistical methods; and (2) develop new, approximate GDF equations to predict live load radial moment distribution in curved bridges.

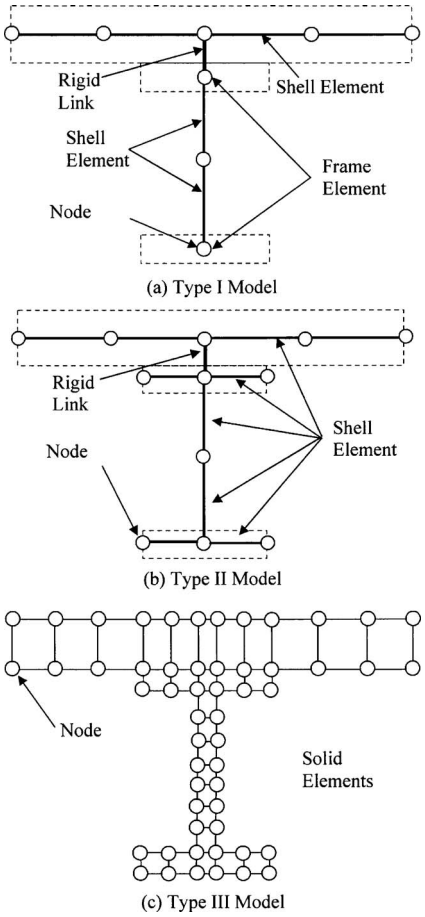

Fig. 1. Levels of analysis

Level of Analysis Study

Prior to initiating the parametric study, a level of analysis study was conducted to establish the numerical modeling methodology. Three levels of three-dimensional numerical models were built using a standard, commercially available software package: (1) frame elements at girder flanges (Type I); (2) shell elements at girder flanges (Type II); and (3) solid elements throughout the entire structure numerical model (Type III). All numerical models included geometric and material properties and support conditions consistent with those observed in normal construction. For purposes of evaluation, curved I-girder bridge response field data collected by McElwain and Laman (2000) were compared to results derived from each level of numerical analysis. For the level of analysis study, three numerical models of increasing complexity and refinement were evaluated for their effectiveness in simulating the behavior observed in a field tested, curved, I-girder bridge (see Fig. 1).

Field Data

McElwain and Laman (2000) conducted field tests of three curved, steel, I-girder bridges to obtain experimentally derived live load distribution factors. The bridge utilized herein for comparative purposes, selected from the three tested bridges by McElwain, is a single-span, four-girder system with girders spaced at 2.44 m (8 ft-0 in.). This bridge was selected because it most closely represents a typical curved girder bridge with few unique characteristics and matches closely the structures to be considered in the present study. The outermost girder has 2.9 m (9 ft-6 in.) straight length and 21.6 m (70 ft-6 in.) curved length with a radius equal to 75.9 m (259 ft-0 in.). The concrete deck slab of the bridge is 216 mm $\left(8\frac{1}{2}\text{ in.}\right)$ and four cross frames are spaced at approximately 5.2 m (17 ft-0 in.).

GDF data collected by McElwain and Laman was used as the basis for evaluation of level of analysis accuracy. Although the field tested bridge has a small skew angle at the abutment, this was not expected to significantly influence GDF predictions based on AASHTO LRFD (2006). Accuracy of the numerical model in predicting the observed response was the criterion for evaluation to select an appropriate numerical model. All geometric conditions of the tested bridge were modeled during the level of analysis study for direct comparison between observed response and numerical response. In addition, axle loads and dimensions of the truck used for the field tests were reproduced in the models.

Level of Analysis Model

The Type I [Fig. 1(a)] model is similar to that employed by Brockenbrough (1986) to examine GDFs in curved bridges. The model was constructed using shell elements for the concrete deck and girder webs, frame elements for the girder flanges and cross frames, and rigid bars to connect girder flanges to the concrete deck. The Type II model, presented in Fig. 1(b), is based on the research by Zureick and Naqib (1999). The main difference between Types I and II is that Type II uses shell elements at girder flanges.

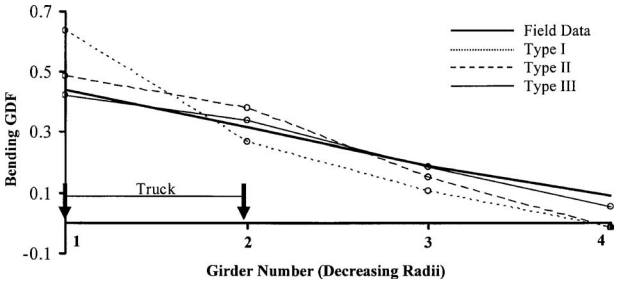

Fig. 2. Representative GDF comparison of field versus numerical data

The Type III model is based on a numerical model used by Yoo and Littrell (1986). This numerical model is composed entirely of 8-node solid elements. As presented in Fig. 1(c), only the cross frames were modeled using frame elements.

As presented in Fig. 2, the Type I model yielded relatively inaccurate GDFs (45%) from field experimental values and was, therefore, eliminated as a modeling approach. Type II and Type III models demonstrated better predictions of GDFs where the differences compared to field tested results were only 10 and 4%, respectively. However, Type III models require significant development effort, particularly in the present study where 81 cases are considered. Therefore, it was determined that the Type II numerical model was most appropriate for use in the present study.

Parametric Study

To initiate the parametric studies, 81 curved, I-girder bridges were designed using commercially available software (DESCUS) in accordance with load factor design (LFD) specifications from the *AASHTO Guide* (2003). A typical bridge section and plan for this study are presented in Fig. 3. Due to limited resources for the design of 81 bridges, the same girder section was used for all four girders in a given bridge. Impact factors for LFD and load combinations were taken from *AASHTO Guide* (2003).

Parameters

The maximum total bending of a curved girder is composed of strong-axis bending and weak-axis warping normal stresses. The parametric study included radius, span length, girder spacing, and cross-frame spacing. The influences of other parameters on GDFs, such as parapets, girder flange width, web depth, and deck thickness were also investigated. These parameters were found to insignificantly influence GDFs and were excluded from the GDF equations reported herein (Kim 2004).

To investigate the influence of radius of curvature on GDFs, small, medium and large radii were selected. *AASHTO Guide* (1993) suggested four ranges of radii corresponding to different cross frame spacings: (1) less than 61 m (200 ft); (2) 61–152 m (200–350 ft); (3) 152–305 m (350–1,000 ft); and (4) larger than 305 m (1,000 ft). Although the less than 61 m (200 ft) radius is seldom used for practical curved highway bridges, a 61 m (200 ft) outer girder radius was selected to evaluate the effect of severe curvature. A radius of over 305 m (1,000 ft) was excluded from this study because a radius of this magnitude approaches straight girder bridge behavior according to *AASHTO Guide* (2003) criteria. The four radii ranges found in *AASHTO Guide* (1993) were utilized to determine medium and small curvature

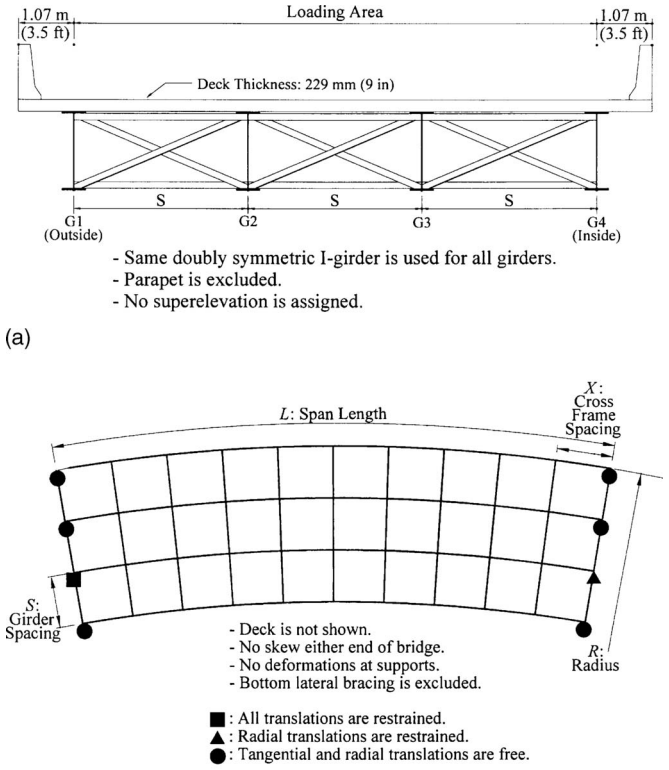

Fig. 3. Parametric study typical bridge cross section and plan: typical bridge (a) cross section; (b) plan

values in the present study: 61, 107, and 229 m (200, 350, and 750 ft) radii of the outer girder.

The span length range of practical single-span curved steel I-girder bridges generally ranges from 15 to 60 m (from 50 to 200 ft). Therefore, the present study adopted 22, 33, and 44 m (72, 108, and 144 ft) span lengths. To equally space cross frames within each of the spans, 2.2, 3.7, and 5.5 m (7.2, 12, and 18 ft) cross-frame spacing was selected. Radial girder spacing was taken as 3.05, 3.35, and 3.66 m (10, 11, and 12 ft) to evaluate the practical spacing of two-lane, curved, I-girder bridges.

Truck Position

To determine the maximum response of the modeled curved bridges to the selected live load model, critical truck positions must be determined. For the present study, two and three AASHTO HS25 trucks and lane loads were applied to the numerical model based on bridge width. Each wheel line or lane load was assumed to conform to the bridge curvature to be on the same curvature because a line of real truck wheels has a similar curvature to the curved bridge.

A trial and error protocol was established for radial truck position to establish critical wheel load paths. HL-93 loadings were systematically placed at 305 mm (1 ft) increments from the outside girder. The determination of truck positions for maximum girder response accounted for both bending and warping normal stresses in the flange of the outside girder. All results reported herein refer to outside girder response. In most cases, the truck position producing maximum bending normal stress was in agreement with maximum total (bending+warping) normal stress. In the cases where the truck position producing maximum bending

normal stresses was different from the position producing the maximum total stress, the total stress difference was less than 1% and the tangential distance between those locations was within 305 mm (1 ft). Results from the protocol indicated an extreme truck position at 610 mm (2 ft) from the outer parapet. Although a trend of variation of truck position could not be observed in this analysis, it was shown that the critical truck positions of long radius curved bridges did not vary as much as that of short radius curved bridges.

For the truck position along the arc, an influence line analysis was used. The expected maximum bending normal stress point on the girder, based on a straight girder analysis, is under the mid-axle located at 711 mm (2 ft-4 in.) from the bridge midspan. However, the location of the actual, curved girder maximum total normal stress was not coincident with this location. The maximum total normal stress for the studied curved girders was strongly related to the cross frame locations because severe normal stress changes were observed at the cross-frame locations. Therefore, the maximum normal stress curved girder response was collected at any points that produced the maximum total normal stress.

GDF Model Formulation

Two methods were employed to determine coefficients for each parameter in the GDF models using the numerical data:

1. Averaged coefficient (AC) method—uses averaged coefficients from all parametric study results to determine each coefficient in the GDF model (Zokaie 2000).
2. Regression analysis (RA) method—uses the least-square method (LSM) to determine each coefficient of the GDF model.

The developed GDF equations include both bending and warping effects to predict maximum total bending response of a curved girder. Also, each of the developed GDF models was classified into two types:

1. Single GDF model (SGM)—The maximum total bending response of curved girders including bending and warping was used to develop a GDF equation.
2. Combined GDF model (CGM)—A maximum sum of bending and warping GDF model is composed of a bending GDF model (CGM-B) and a warping GDF model (CGM-W). CGM-B was derived using the maximum bending normal stress of curved girders and CGM-W was developed using the maximum warping normal stress. After these separate derivations, both GDF models were combined to predict the maximum total bending response of a curved girder.

A model similar to that used by Zokaie was employed in the present study for both AC and RA methods with the basic form

$$g = (a)(R^{b1})(S^{b2})(L^{b3})(X^{b4}) \tag{1}$$

where a=scale factor and $b1$, $b2$, $b3$, and $b4$ are exponents determined by the variations of outside girder radius (R), girder spacing (S), radial span length of the outside girder (L) and cross-frame spacing of the outmost girder (X), respectively. Because each exponent represents the strength of a parameter's correlation, this type of GDF formula is also instructional, indicating the strength of each parameter.

GDF Model

A method similar to Schelling et al. (1989) was employed for the present GDF equation. The GDF concept used in the present study originated from

$$\text{Max. moment per girder in multilane curved bridge} = g \times \text{Max. moment per bridge in one lane straight bridge} \tag{2}$$

where g=GDF. This concept can be rewritten as

$$g = \frac{\text{Max. moment per girder in multilane curved bridge}}{\text{Max. moment per bridge in one lane straight bridge}} = \frac{M_c}{M_s} \tag{3}$$

To promote simplicity in the proposed model, moments from a line girder analysis having the same section properties and span length subjected to one lane of HL-93 loading was used for M_s in Eq. (3). Two methods (SGM and CGM) were considered for M_c in Eq. (3).

Warping Model

Warping normal stress in a curved girder directly affects the total flange normal stress as it is superimposed on bending normal stress. Thus, the maximum total normal stress of a curved girder must include warping normal stress as well as bending stress. Two types of GDF equations were considered that include warping normal stress together with bending normal stress. Whereas SGM was developed from the maximum total normal stress of a curved girder, CGM used maximum bending normal stress and maximum warping normal stress. In the CGM, CGM-B for maximum bending normal stress and CGM-W for maximum warping normal stress were developed separately. Then the total GDF model was formed using the combination of both bending and warping GDF models.

Single GDF Model

The maximum total normal (resultant) stress obtained from the 81 numerical models was used to determine the curved girder vertical bending moment (M_c). Sections were taken as composite and the maximum moment was calculated from $f_{\text{normal}}=M_c y/I_{x,\text{composite}}$. The resulting SGM GDF can be presented as

$$g_{B+W} = \frac{M_{C(B+W)}}{M_S} = \frac{f_{(\text{GDR})(B+W)} I/y}{M_S} \tag{4}$$

where $g_{(B+W)}$=GDF; $M_{C(B+W)}$=maximum moment including bending and warping; $f_{(GDR)(B+W)}$=maximum normal stress in the curved girder; I=x-axis bending moment of inertia of the composite cross section based on the effective slab width; y=vertical distance from the elastic neutral axis of the section; and M_S=maximum bending moment of the straight bridge model of identical length. This GDF can be used to calculate the maximum girder moment as

$$\text{Max } M_c = g_{(B+W)} M_s \tag{5}$$

where Max M_c=maximum total moment in the curved girder and M_s=straight bridge maximum moment.

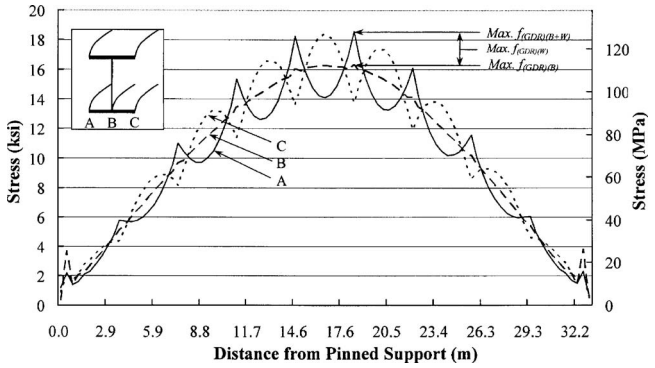

Fig. 4. Tangential normal stress variation, Girder 1, Analysis Case 41

Combined GDF Model

Regression based GDF formulas, enabling the determination of total stresses can be derived separately in a bending normal stress model and warping normal stress model. However, it was observed that the tangential location of the maximum bending normal stress is not always coincident with the maximum total normal stress (i.e., sum of bending and warping stresses). This inconsistency is a consequence of cross frame and girder interaction when resisting applied loads, as shown in Fig. 4 for analysis Case 41 with warping normal stresses superimposed on bending normal stresses along the span. Therefore, maximum bending normal stress was used for CGM-B and maximum warping normal stress irrespective of its location along arc span was adopted for CGM-W. As an example, Case 41 (Fig. 4) has cross frames spaced at 3.7 m (12 ft) intervals in a 33 m (108 ft) arc span length. The analysis results indicate that the maximum stress location by influence line analysis does not correspond with maximum total normal stress location where a cross frame or midpoint of two cross frames occurs. The maximum flange total normal stress was appreciably affected by cross frame restraint as observed by discontinuities in the normal stresses.

The proposed GDF models are intended to determine the preliminary girder design moments based on a line girder analysis, a commonly used preliminary design method. Because vertical bending moment is the only moment obtained from a line girder analysis, warping effects were accounted for by modifying the line girder vertical bending moments. The normal stresses due to both bending and warping act in the same direction. Therefore, the maximum warping moment was transformed into an equivalent vertical bending moment based on the magnitude of the warping stress. This transformation allows prediction of maximum warping stress based on the 81 sample curved bridge design data.

Warping normal stress was calculated by subtracting the bending normal stress from the maximum total normal stress obtained from the computer analyses. CGM-B was determined using

$$g_B = \frac{M_{C(B)}}{M_S} = \frac{f_{(\mathrm{GDR})(B)} I/y}{M_S} \tag{6}$$

where g_B=vertical bending GDF; $M_{C(B)}$=maximum vertical bending moment; and $f_{(GDR)(B)}$=maximum bending normal stress in a curved girder. The CGM-W has been calculated as

$$g_W = \frac{M_{C(W)}}{M_S} = \frac{(f_{(\mathrm{GDR})(B+W)} - f_{(\mathrm{GDR})(B)}) \cdot I/y}{M_S} \tag{7}$$

where g_W=warping GDF; $M_{C(W)}$=equivalent maximum warping moment in the curved girder; and $f_{(GDR)(B)}$=bending normal stress at maximum total normal stress location. Therefore, the final GDF by CGM was obtained from

$$g_{B+W} = g_B + g_W \tag{8}$$

During an actual curved bridge design, the required maximum girder moment can be estimated using a SGM approach with Eq. (5). Alternatively, bending and warping moments for a curved girder can be determined separately using a CGM approach with Eqs. (6) and (7). In addition, the separate two terms (g_B and g_W) in CGM are useful for the 1/3rd rule equation by AASHTO LRFD (2006). Based on results of the parametric study, GDF equations were developed using both the previous methods.

Discussion of Results

Parametric Effect

Normal stresses, girder moments and corresponding GDFs for each parametric study case were evaluated. Both bending and warping normal stresses were evaluated separately to determine the largest normal stress response. Maximum girder total bending moments calculated from the bending normal stress and the bending plus warping normal stress for the outside girder for all 81 cases are presented in Fig. 5. Equivalent warping moment had a large influence on the total bending moment. The inclusion of warping normal stresses increases the girder total moment by 2–29% over the vertical bending moment and this effect is more significant as span increases and radius decreases. As anticipated, for all spans lengths and radius, warping normal stresses increase as cross frame spacing increases. Figures 6–8 examine the influence of each of the four key parameters on the radial moment distribution.

As observed from the data presented in Fig. 6, GDFs obtained directly from the numerical analyses generally increase as cross frame spacing increases for a given span length. Warping normal stress variations are primarily responsible for this trend. It can also be observed from Fig. 6 that girder spacing, for the range considered, does not strongly influence GDFs as compared to span length. However, it is anticipated that girder spacing over a wider range will significantly influence radial moment distribution and should be maintained as a parameter in the final GDF equations (*AASHTO Guide* 1993; Brockenbrough 1986; Schelling et al. 1989; Sennah and Kennedy 1999). The data in Fig. 6 also indicates that GDFs decrease as radius increases, most notably for longer spans [Fig. 6(c)].

The data presented in Fig. 7, derived from numerical analysis indicate that GDF is strongly influenced by span length, particularly for a shorter radius. At a radius of 61 m (200 ft), GDF increases between 38 and 100% over the range of cross frame spacing considered. The GDF also significantly decreases as radius increases and this parameter significantly affects the influence of all other parameters on GDFs. The influence of span length on GDF is affected by radius length, particularly as a result of increasing warping stress. As observed in Figs. 7(a–c), at a radius of 229 m (750 ft) the effect of span is very small, changing the GDF by no more than 10% over the range of cross-bracing spacing and span lengths considered.

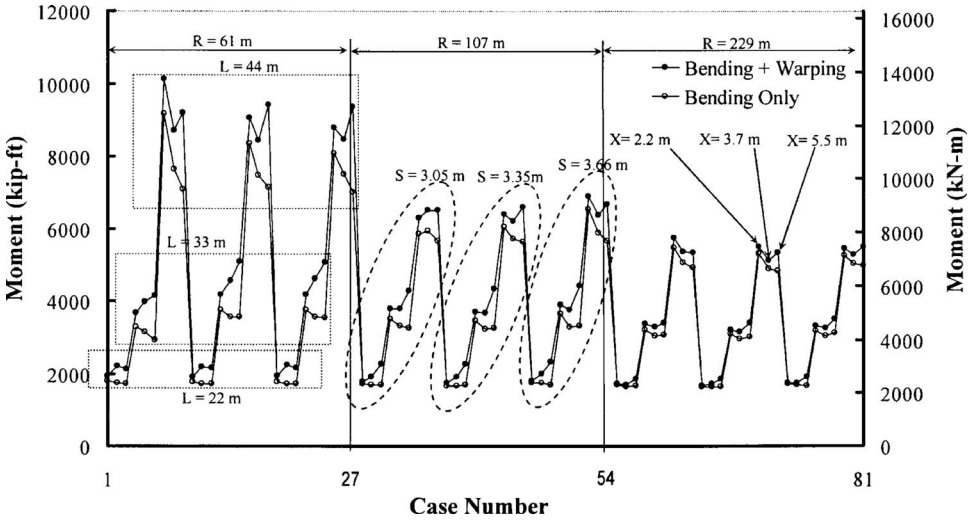

Fig. 5. Maximum moment for outside girder, parametric studies

Fig. 8 indicates a strong correlation between L/R ratio and GDFs. GDFs converged to approximately 1.0 as the ratio approaches zero, irrespective of girder spacing.

Strength of Each Parameter

The GDF model format presented in Eq. (1) was adopted for both the AC and RA methods. The strength of each parameter on the final GDF value is easily recognized by the coefficient of each variable (i.e., $b1$, $b2$, $b3$, and $b4$ directly correspond to the strength of R, S, L, and X). As a preliminary step in determining GDF model coefficients, variables that did not strongly or consistently influence the GDFs from the numerical analyses were eliminated from both the AC and RA methods. Specifically, both girder and cross frame spacing for CGM-B and solely girder spacing for SGM and CGM-W were excluded for the AC method because their variations were errant. For example, the coefficients of girder spacing for SGM, CGM-B, and CGM-W ranged from −1.15 to 2.13, from −0.99 to 2.04, and from −3.90 to 2.37, respectively, which is an extremely wide range.

For the RA method, a P-value test was conducted twice with a 95% confidence interval to obtain GDF coefficients. The first trial of the RA method included all parameters. In the second, trial parameters that were deemed insignificant ($P > 0.05$) were excluded. The variables eliminated in the RA method are the same as those eliminated in the AC method. Because these eliminated variables are shown not to be important for a GDF model, R^2 was not significantly affected (0.2%). The final coefficients of each parameter corresponding to Eq. (1) are presented in Table 2. The results indicate that span length has the most significant influence on CGM-B (71.2% in RA method) and CGM (49.4% in RA method). Cross-frame spacing also significantly influences CGM-W (49.5% in RA method) and CGM (14% in RA method).

Accuracy of Proposed Models

A goodness-of-fit test was utilized to determine the most accurate GDF model among four developed equations (SGM and CGM by AC method and SGM and CGM by RA method). The four GDF models in Table 2 produced very similar results to each other. SGM by the AC method predicts slightly higher GDFs and total bending moments when compared to numerical GDFs. Conversely, CGM by the AC method predicts slightly lower GDFs and total bending moments. However, GDF models by the RA method presented in Figs. 9–11 predicted GDF values very close to numerically derived GDFs. To determine the accuracy of the four GDF models, R^2 was calculated and is presented in Table 3. It can be observed from Table 3 that R^2 values larger than 1.0 were calculated, which cannot exist in theory. Therefore, the predicting model represents a different distribution from that which it was intended to predict (Devore 2000). For this reason, the AC method was determined to be inappropriate for the calculation of GDFs for curved bridges.

In contrast to the AC method, the RA method resulted in reasonable R^2 values (less than 1.0) as presented in Table 3. The LSM used for the RA method sought optimized coefficients that maximized R^2 values less than but possibly close to 1.0. In the present study, CGM presented a better R^2 (=92.5%) than SGM (=77.2%). In addition, the RA method CGM provides vertical bending moments and equivalent warping moments separately because the model consists of two separate equations. Therefore, the RA method CGM was selected as the most accurate GDF equation among the four equations and presented in

$$g_{B+W} = (0.373R^{-0.14}L^{0.35})_{\text{bending}} + (0.112R^{-0.94}L^{0.38}X^{1.3})_{\text{warping}} \tag{9}$$

The proposed GDF equation, the RA method CGM, was compared to the *AASHTO Guide* (1993) GDF equation and numerical model results as presented in Fig. 9. It is noted that *AASHTO Guide* (1993) GDF equation not a function of L/R alone, therefore, was plotted with respect to three studied radii. The *AASHTO Guide* (1993) equation presented herein incorporates the modification factor equation found in *AASHTO Guide* (1993). The *AASHTO Guide* (1993) equation predicted much higher GDFs compared to numerically derived GDFs, especially for both radius equal to 229 m (750 ft) cases and large central angle cases, while the proposed GDF equation produced a close match to the parametric study results.

Applying the proposed GDF model, the predicted GDFs and maximum total moments for the outer girder in the 81 cases are presented in Figs. 10 and 11, respectively. The accuracy of each model for the CGM-B and the CGM-W is presented in Table 3. The CGM-B and the CGM-W precisely predict bending GDFs

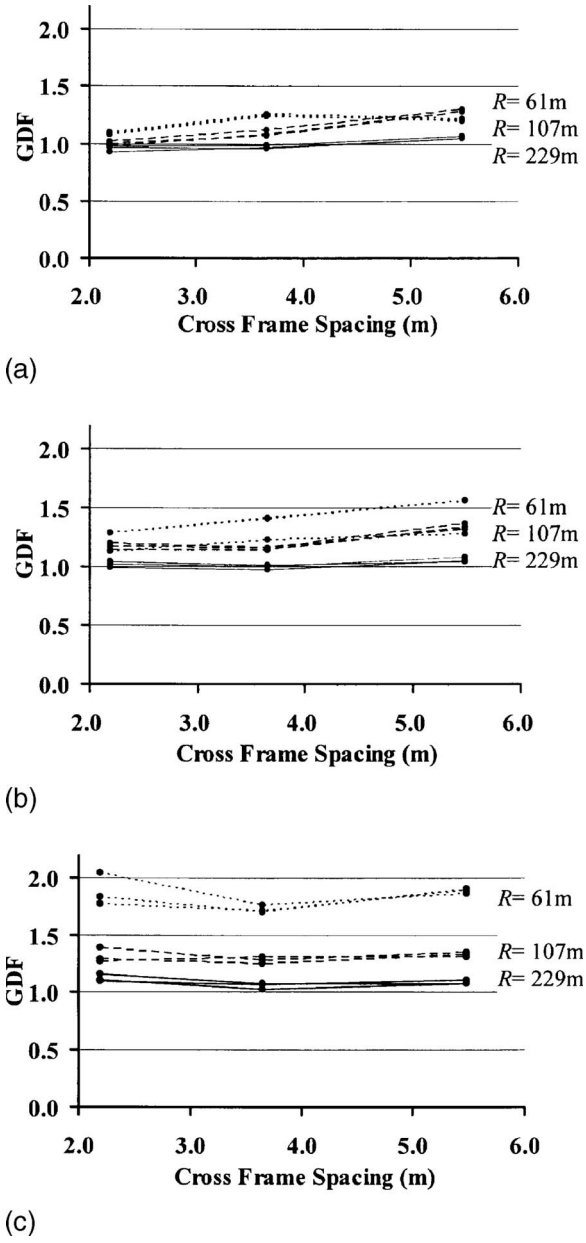

Fig. 6. Effect of cross frame spacing and radius on GDF, S=3.1, 3.4, and 3.7 m (10, 11, and 12 ft), respectively; L=(a) 22 m (72 ft); (b) 33 m (108 ft); and (c) 44 m (144 ft)

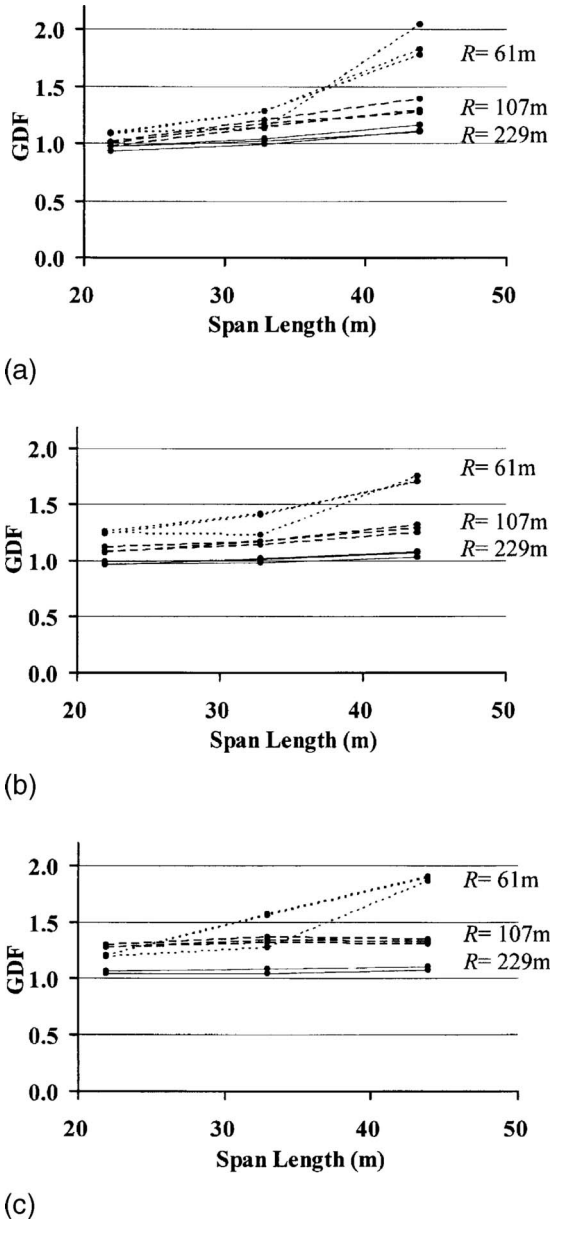

Fig. 7. Effect of span length and radius on GDF, S=3.1, 3.4, and 3.7 m (10, 11, and 12 ft), respectively: X=(a) 2.2 m (7.2 ft); (b) 3.7 m (12 ft); and (c) 5.5 m (18 ft)

and moments in the cases of radius 107 m (350 ft) and 229 m (750 ft) and warping GDFs and moments in all cases of interest, respectively.

Conclusions

Live load radial moment distribution in curved I-girder bridges was investigated using a numerical parametric study and a GDF model to predict GDFs was developed using statistical methods. The following conclusions were derived from the present research.

Numerical models, evaluated on the basis of observed field behavior, were employed to simulate curved I-girder bridge behavior under live load. Type I numerical models incorporating frame elements at girder flanges over-predicted the response by 45%. Type II numerical models incorporating shell elements at flanges were in good agreement (10% difference) with GDFs based on field measurements. Type III numerical models produced more accurate results than those of Type II, however, the level of effort for this model was excessive. Numerical models of Type II are recommended for acceptably accurate analysis of curved I-girder bridges.

The parameters that most significantly influence radial live load distribution in curved, I-girder bridges are radius, span length, cross frame spacing and girder spacing. Radius, span length, and cross-frame spacing are strongly related to the maximum bending and/or warping GDFs of curved bridges. Parapet, deck thickness, flange width and web depth have a small and relatively insignificant influence on GDFs compared to key parameters.

Bending and warping effects on GDFs have been determined.

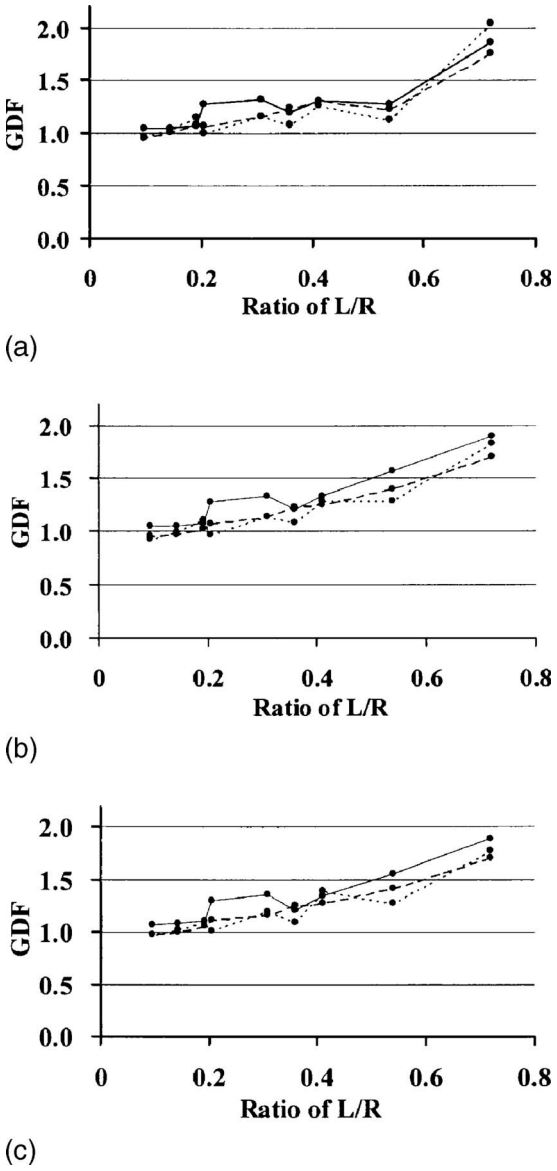

Fig. 8. Effect of L/R ratio on GDF, S=(a) 3.05 m (10 ft); (b) 3.35 m (11 ft); and (c) 3.7 m (12 ft)

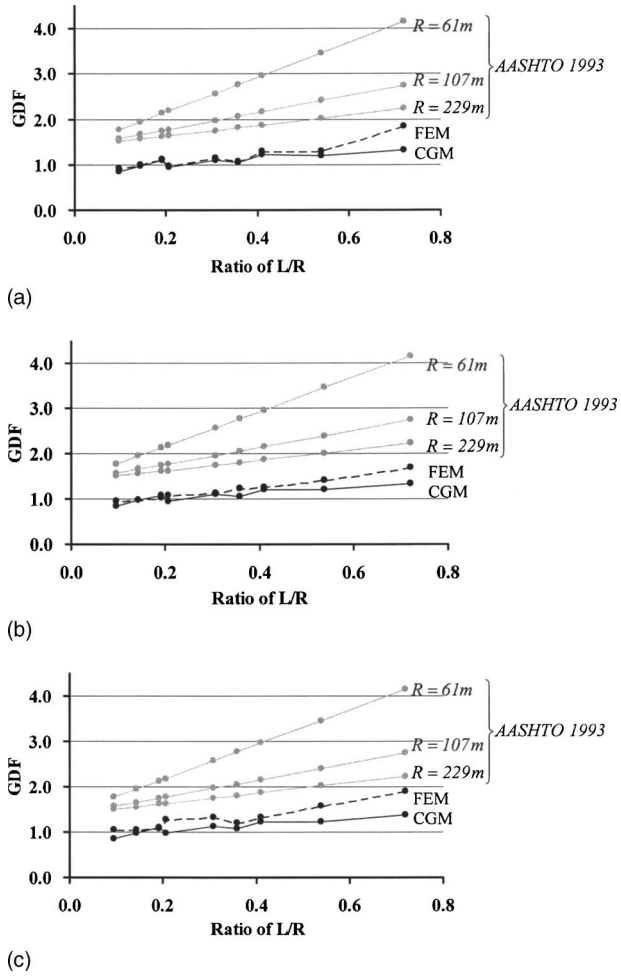

Fig. 9. GDF comparisons [S=3.4 m (11 ft)]: X=(a) 2.2 m (7.2 ft); (b) 3.7 m (12 ft); and (c) 5.5 m (18 ft)

The bending effect on GDFs increases as span length increases. The warping effect on GDFs increases as the radius decreases. For a short radius [R=61 m (200 ft)], warping effects on GDFs of an outside girder significantly increased compared to bending response. For the present study, the largest ratio of warping normal stress to bending normal stress was 43%. However, the normal stress ratio (14%) of warping to bending was comparatively small for a 229 m (750 ft) radius.

The most influential parameter on the total bending GDFs is span length. Cross-frame spacing and girder spacing inconsistently influenced bending GDFs within the scope of the present study. However, cross-frame spacing was the dominant parameter for warping GDFs.

The proposed GDF equation for curved I-girder bridges proposed by the present study is accurate and simple to apply for preliminary design. The proposed approximate GDF equation produces high accuracy (R^2=92.5%) against the numerically de-

Table 2. Coefficients of GDF Formulas

Method	Equation type		GDF	Coefficient				
				a	$b1$	$b2$	$b3$	$b4$
AC	SGM		$g_{(B+W)}$	0.548	−0.248	—	0.357	0.103
	CGM	CGM-B	$g_{(B)}$	0.307	−0.151	—	0.412	—
		CGM-W	$g_{(W)}$	0.103	−0.933	—	0.362	1.308
RA	SGM		$g_{(B+W)}$	0.723	−0.240	—	0.324	0.092
	CGM	CGM-B	$g_{(B)}$	0.373	−0.143	—	0.354	—
		CGM-W	$g_{(W)}$	0.112	−0.942	—	0.378	1.294

Note: a, $b1$, $b2$, $b3$, and $b4$=coefficients of $g=(a)(R^{b1})(S^{b2})(L^{b3})(X^{b4})$. All coefficients correspond to S.I. unit (m).

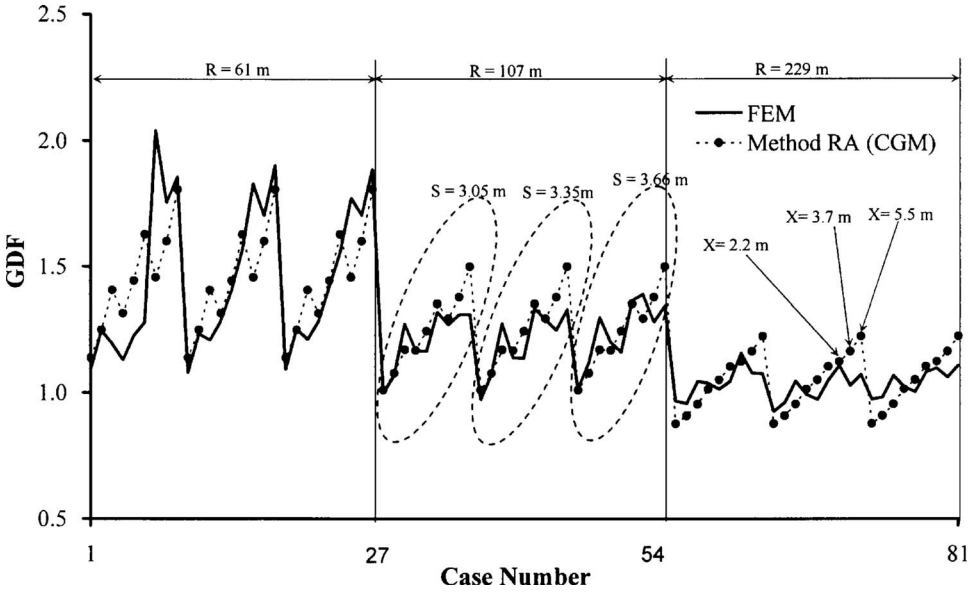

Fig. 10. GDF predictions using Method RA CGM

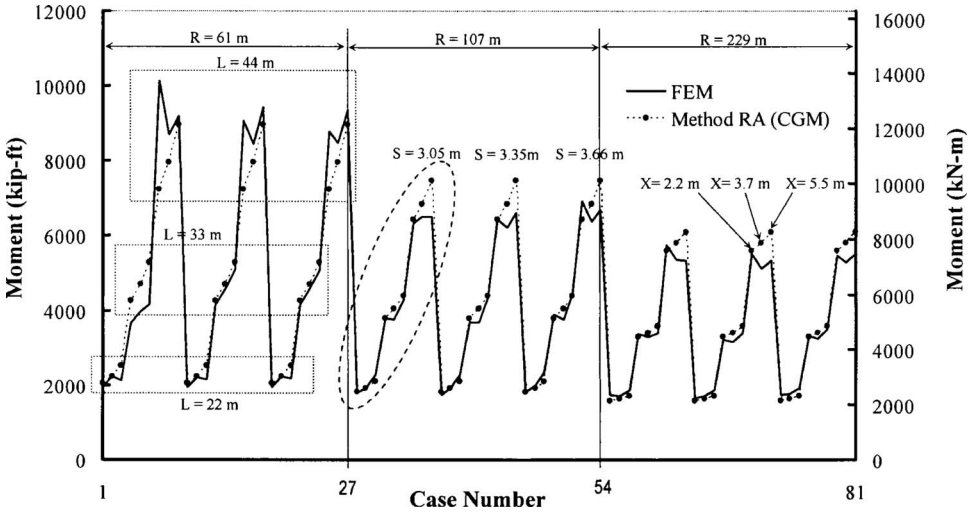

Fig. 11. Maximum total moment using Method RA CGM

rived GDFs. The equation predicts well for curved steel I-girder bridges with a 61–229 m (200–750 ft) radius, 22–44 m (72–144 ft) span length, 2.2–5.5 m (7.2–18 ft) cross frame spacing, and 3.05–3.66 m (10–12 ft) girder spacing. In particular, the proposed equation as applied to 107–229 m (350–750 ft) radii resulted in very accurate predictions.

Table 3. Comparison of R^2

Method	Equation	GDF	R^2
Method AC	SGM	$g_{(B+W)}$	1.149
	CGM-*B*	$g_{(B)}$	1.133
	CGM-*W*	$g_{(W)}$	0.935
	CGM	$g_{(B+W)}$	1.139
Method RA	SGM	$g_{(B+W)}$	0.772
	CGM-*B*	$g_{(B)}$	0.652
	CGM-*W*	$g_{(W)}$	0.928
	CGM	$g_{(B+W)}$	0.925

Notation

The following symbols are used in this paper:

a = scale factor;
b = coefficient ($b1$, $b2$, $b3$ and $b4$);
f = stress;
g = girder distribution factor;
I = moment of inertia of the composite cross section
L = span length of outside girder;
M = moment;

R = radius of outside girder;
R^2 = determination of coefficients for a goodness-of-fit test;
S = girder spacing;
X = cross frame spacing of outside girder; and
y = vertical distance from the elastic neutral axis.

Subscripts

B = bending response;
BRG = bridge;
$B+W$ = total (bending and warping) response;
C = curved girder bridge;
GDR = girder;
S = straight girder bridge; and
W = warping response.

References

American Association of State Highway and Transportation Officials (AASHTO). (1993). *Guide specifications for horizontally curved highway bridges*, Washington, D.C.

American Association of State Highway and Transportation Officials (AASHTO). (2003). *Guide specifications for horizontally curved highway bridges*, Washington, D.C.

American Association of State Highway and Transportation Officials (AASHTO). (2006). *AASHTO LRFD bridge design specifications*, Washington, D.C.

Brockenbrough, R. L. (1986). "Distribution factors for curved I-girder bridges." *J. Struct. Eng.*, 112(10), 2200–2215.

Devore, J. L. (2000). *Probability and statistics for engineering and the sciences*, 5th Ed., Duxbury of Thomson Learning, 277–353.

Kim, W. (2004). "Live load radial moment distribution for horizontally curved I-girder bridges." MSc thesis, The Pennsylvania State Univ., University Park, Pa.

McElwain, B. A., and Laman, J. A. (2000). "Experimental verification of horizontally curved I-girder bridge behavior." *J. Bridge Eng.*, 5(4), 284–292.

Schelling, D., Namini, A. H., and Fu, C. C. (1989). "Construction effects on bracing on curved I-girders." *J. Struct. Eng.*, 115(9), 2145–2165.

Sennah, K., and Kennedy, J. B. (1999). "Simply supported curved cellular bridges: Simplified design method." *J. Bridge Eng.*, 4(2), 85–94.

Yoo, C. H., and Littrell, P. C. (1986). "Cross-bracing effects in curved stringer bridges." *J. Struct. Eng.*, 112(9), 2127–2140.

Zokaie, T. (2000). "AASHTO-LRFD live load distribution specifications." *J. Bridge Eng.*, 5(2), 131–138.

Zureick, A., and Naqib, R. (1999). "Horizontally curved steel I-girders state-of-the-art analysis methods." *J. Bridge Eng.*, 4(1), 38–47.